

# Adaptive Phase and Ground Quadrilateral Distance Elements

Fernando Calero, Armando Guzmán, and Gabriel Benmouyal, *Schweitzer Engineering Laboratories, Inc.*

**Abstract**—Quadrilateral distance elements can provide significantly more fault resistance coverage than mho distance elements for short line applications. Quadrilateral phase and ground distance element characteristics result from the combination of several distance elements. Directional elements discriminate between forward and reverse faults, while reactance and resistance elements are fundamental to the proper performance of the quadrilateral characteristic. Load flow considerations determine the choice of the polarizing quantity for these elements. Reactance elements must accommodate load flow and adapt to it. Resistive blinders should detect as much fault resistance as possible without causing excessive overreach or underreach of the quadrilateral distance element. In this paper, we discuss an adaptive quadrilateral distance scheme that can detect greater fault resistance than a previous implementation. We also discuss application considerations for quadrilateral distance elements.

## I. OVERVIEW

Whereas the literature debates the differences and benefits of mho and quadrilateral ground distance elements [1], this paper describes the theory, application, and characteristics of a particular implementation of phase and ground quadrilateral distance elements.

It is well accepted that a quadrilateral characteristic is beneficial when protecting short transmission lines [1][2]. It is also accepted that sensitive pilot protection schemes do not rely on distance elements only; these schemes also rely on ground directional overcurrent (67G), a unit that provides higher fault resistance ( $R_f$ ) detecting capabilities than ground distance elements of any shape [3].

Generally, high  $R_f$  faults have been associated with single-line-to-ground faults (AG, BG, CG). For these faults, the associated  $R_f$  is considerable. On the other hand, phase faults are less susceptible to high  $R_f$  values. However, because short transmission lines are much more affected by high  $R_f$  values, the element with the most fault detecting capabilities should be used [1][2][3].

### A. Fault Resistance

Short circuits along the transmission line will have some degree of additional impedance. If this additional impedance is negligible, the line impedance is prevalent, and the apparent impedance measured will reflect it by reporting an impedance with the same angle as the line impedance. On the other hand, if this additional impedance is not negligible, the measured apparent impedance no longer appears at the line angle.

Fig. 1 shows the different components of fault resistance for transmission line faults. Although extremely simplified, the figure shows the phase conductors (only Phase A and

Phase B are shown), the tower structure, the insulator chains, the ground wire, and the different impedances to the flow of fault current. These impedances are simplified to be resistive values only [4][5].

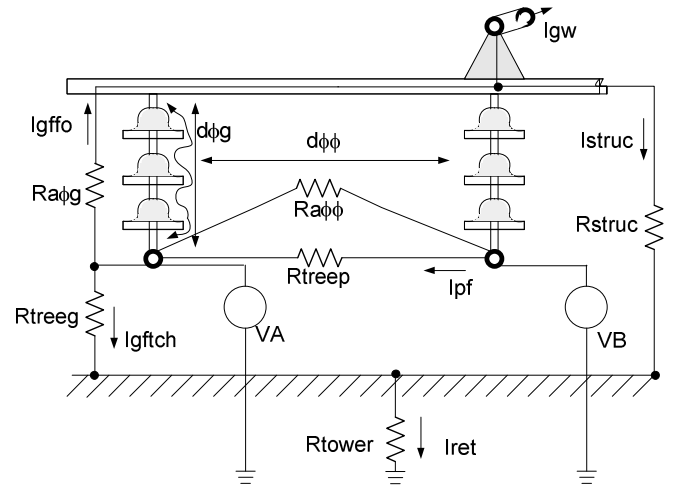


Fig. 1. Visualizing the  $R_f$  component

The  $R_{tower}$  resistance is generally called the “footing resistance.” It is a critical parameter regarding the design and construction of transmission lines [6]. For an insulation flashover fault, the return path is through the tower itself. When a foreign object touches the conductors, the current distributes between adjacent towers but returns through the footing resistance. Ideally, the smaller the footing resistance, the better the transmission line ground fault detection performance will be. However, even though smaller values exist, practical values range from 5 to 20 ohms; and in rocky terrain, the resistance could be 100 ohms or more [1].

In Fig. 1,  $R_{a\phi g}$  represents the arc resistance for an insulator flashover for a phase-to-ground fault. This is in the path of the ground fault flashover current  $I_{gffo}$ .  $R_{a\phi\phi}$  is the arc resistance for a phase-to-phase fault.

The arc resistance value is dependent on the arc length and the current flowing through the arc. A well-accepted formula is the one empirically derived by A. Van Warrington, expressed in (1). Other equations yield similar results [7]. In (1), the arc length is expressed in meters.

$$R_{arc} = 28688.5 \frac{\text{length}}{I^{1.4}} \Omega \quad (1)$$

The arc initially presents a few ohms of impedance. Over time, it could develop into 50 or more ohms [1]. Importantly, its value is dependent on the arc length and the current

flowing through the arc. In Fig. 1, the arc length is denoted as  $d\phi g$  for ground faults and  $d\phi\phi$  for phase faults.

$R_{struc}$  is the tower structure resistance. Although insignificant for a metallic structure, this resistance may carry a significant value if built from a nonconductive material like wood.

$R_{treeg}$  and  $R_{treep}$  are the resistances of foreign objects that could be causing a power system fault. A tree is chosen as an example. These resistance values could be a few hundred ohms.

### 1) Phase-to-Ground Faults

Phase-to-ground faults are the most common type of faults in the power system. They involve a single phase that conducts fault current to ground. There are two possible single-phase-to-ground fault scenarios: insulator flashover and an object creating a path to ground.

#### a) Insulator Flashover

An insulator flashover (arc resistance  $R_{a\phi g}$ ), which may be due to a lightning strike or any other event that would stress the insulator, conducts fault current from the phase conductor to the tower structure ( $I_{gffo}$ ) and then to ground through the “tower footing resistance” ( $R_{tower}$ ). The arc forms on the  $d\phi g$  length. This length is the “creepage distance” of the insulator string, which is the shortest electrical distance between the conductor and the tower measured along the insulator string structure.

#### b) Ground Fault Through an Object

Another possible phase-to-ground fault may occur when the phase conductor contacts an object, such as a tree ( $R_{tree}$ ), which is in contact with ground (see Fig. 1). The contact is most likely not at the tower location. It could occur any place along the span from one tower to another tower. The fault current distributes to ground through the tower resistances, with a larger percentage of current flowing to the footing resistance of the closer tower. Conservatively, we can assume that current is only flowing through a single tower footing resistance. This simple assumption contrasts with other advanced and accurate analysis techniques [8].

Regardless of the two possible scenarios, the path to ground involves the equivalent  $R_{tower}$ , which is the resistance of the composite path from earth to system ground. For an insulator flashover,  $R_f$  is the sum of  $R_{a\phi g}$  and  $R_{tower}$ , ignoring the tower resistance ( $R_{struc}$ ). For a ground fault occurring because of contact with an object to ground,  $R_f$  is the sum of  $R_{treeg}$  and  $R_{tower}$ . The  $R_f$  component for this type of fault can be significant.

The presence of ground wires in the tower distributes the fault current differently. A portion of the fault current will return to ground ( $I_{gw}$ ) through these wires. The ground wires are part of the zero-sequence impedance and therefore not associated to  $R_f$ .

### 2) Phase-to-Phase Faults

Phase-to-phase faults, as Fig. 1 illustrates, do not involve the ground return path. As with phase-to-ground faults, an insulator flashover or phase-to-phase connection through an object could be the cause of the fault.

If the fault is due to insulation flashover,  $R_f$  is expressed by (1), and the arc length could be a straight line or a path around the tower ( $d\phi\phi$ ). The important factor is that  $R_f$  is fully due to the arc resistance.

Because of the spacing between phases in high-voltage (HV) and extra-high-voltage (EHV) transmission networks and even in subtransmission levels, it is highly improbable that an object could produce a phase-to-phase fault because of contact. However, in distribution networks, phase-to-phase faults have a higher probability of occurrence because the conductor can have contact with different objects, like tree branches, flying debris, etc.

### B. The Need for a Quadrilateral Element in Transmission Networks

The following three conclusions can be made based on Fig. 1:

- The arc component of the fault,  $R_{a\phi g}$  or  $R_{a\phi\phi}$ , has a value that can be estimated. Equation (1) indicates that the value may not be significant for transmission levels.
- Ground faults may have significant values of  $R_f$ . The tower footing resistances or foreign object resistances can have large values.
- Phase faults in transmission networks will most likely have a small arc resistance.

When discussing protective distance relaying for transmission lines, it is of interest to understand the relay impedance characteristics and schemes used. Per the discussion above, ground distance relaying for short lines, which can be complicated, benefits from the use of a quadrilateral characteristic because ground faults involve more than the arc resistance. Phase distance relaying, on the other hand, detects faults where only the arc resistance is involved, and therefore the complications of a quadrilateral element are not generally required. For these reasons, protective relaying distance schemes that implement mho phase distance algorithms to detect phase faults and a combination of mho and quadrilateral ground distance elements to detect ground faults are justified.

For the majority of transmission line applications, from subtransmission to EHV voltage levels, the mho phase element and mho quadrilateral ground distance scheme have proven to be adequate. Extremely short lines may be a challenge to this scheme. Zero-sequence and negative-sequence directional overcurrent elements have proven to be the solution for distance element limitations for short lines.

### C. Short Line Applications

A short transmission line will generally have low-impedance and short length values. On an R-X diagram, like the one shown in Fig. 2, the line impedance is electrically very far from the expected maximum load. For some applications, the line impedance reach ( $Z_{set}$ ) values challenge the measurement accuracies of the relay itself.

Even for a ground fault with no arc resistance ( $R_{a\phi g}$  equals zero), the  $R_f$  component will have the value of the tower footing resistance, as discussed previously. Mho ground elements have an intrinsic ability to expand and accommodate more  $R_f$ . This expansion is proportional to the source impedance ( $Z_s$ ), as shown in Fig. 2 [9]. However, if the tower footing resistances are in the range of the line impedances, which add to  $R_f$ , the mho element will have difficulty detecting faults even with no arc resistance. The situation is negatively amplified if the source behind the relay is very strong—implying a very small  $Z_s$ .

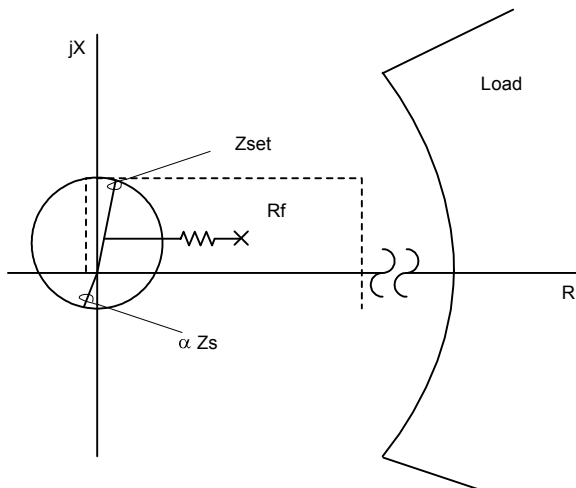


Fig. 2. Short line apparent impedance

Quadrilateral ground distance elements can provide a larger margin to accommodate  $R_f$ . These elements are better suited to protect short lines. There are some limitations in the amount of  $R_f$  that they can accommodate (see Section IV). Nevertheless, their performance is better than that of a mho circle.

The situation for phase fault detection is similar to that of ground fault detection in short line applications. If the expected arc resistance is approximately the same magnitude as the transmission line impedance, the mho phase circle will experience problems detecting the fault. In significantly short line applications, quadrilateral phase distance elements provide notably better coverage than a mho phase element.

Nevertheless, it is accepted that directional overcurrent elements are the most sensitive fault detecting elements and should be included in pilot relaying schemes [1][3].

### D. Directional Overcurrent

Directional overcurrent protection is a more sensitive fault detecting technique than any type of distance element [1][10]. The reach of these elements varies with the source impedance of a transmission network. Ground directional elements are polarized with zero-sequence or negative-sequence voltage. Negative-sequence polarization is also used for phase directional overcurrent protection. Other phase directional schemes are also possible.

In line protection schemes, directional overcurrent is used as a backup scheme for pilot channel loss.

Because pilot relaying schemes offer a directional comparison of the direction to the fault between two or more terminals, it is highly recommended to include the necessary directional overcurrent element (67) with the traditional distance element (21), as illustrated in Fig. 3.

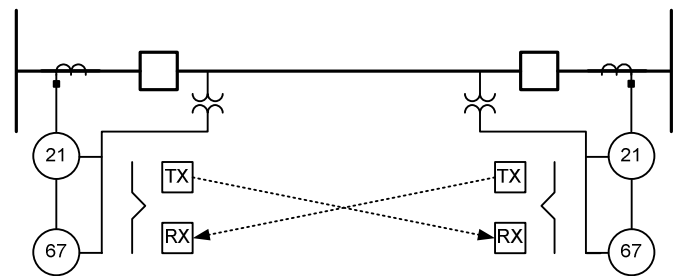


Fig. 3. Directional comparison with directional overcurrent elements

Pilot schemes for ground directional overcurrent, as shown in Fig. 3, will make up for any lack of sensitivity of mho elements for short lines. In fact, greater sensitivity is achieved by using directional overcurrent elements in the scheme, regardless of the types of line and distance elements.

### E. Fault Resistance on the Apparent Impedance Plane

Relay engineers use the apparent impedance plane to analyze distance element performance during load, fault, and power oscillation conditions, either with mho or quadrilateral elements. In this plane, we can represent the apparent impedance for line faults with different values of  $R_f$  and line loading conditions. Fig. 4 shows the system that we used to calculate the apparent impedance for phase-to-ground faults at 85 percent from the sending end.

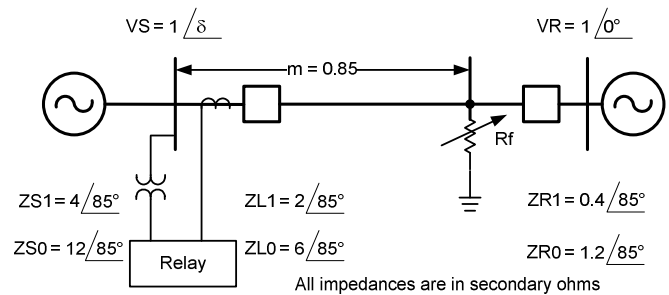


Fig. 4. Power system parameters and operating conditions to analyze the performance of distance elements

Fig. 5 shows the apparent impedance locus for different loading conditions ( $\delta$  equal to  $-20, -10, 0, 10,$  and  $20$  degrees) and all possible values of  $R_f$ .

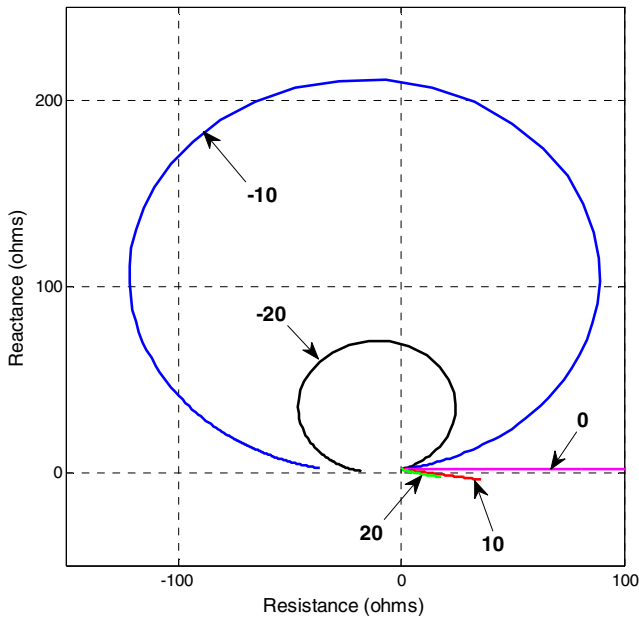


Fig. 5. Apparent impedance for  $\delta$  equal to  $-20, -10, 0, 10,$  and  $20$  degrees while  $R_f$  varies from  $0$  to  $\infty$

Fig. 6 shows that the apparent impedance can cause distance elements with fixed characteristics over- and underreach and have limited  $R_f$  coverage if the distance element does not have an adaptive characteristic [11].

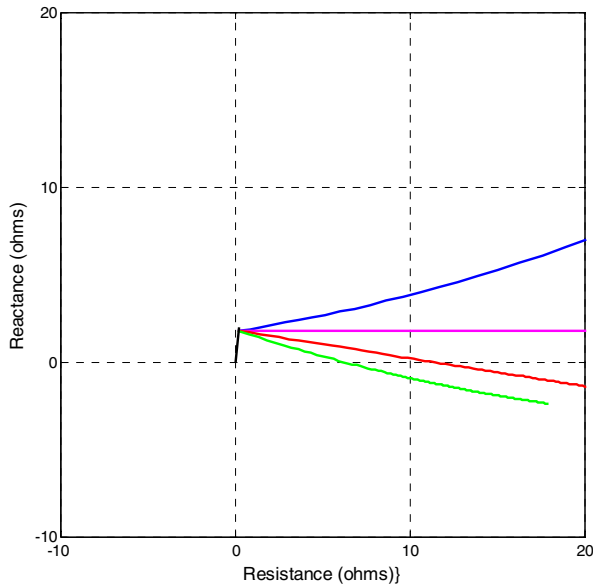


Fig. 6. Apparent impedance can cause distance element over- and underreach and have limited  $R_f$  coverage

Fig. 7 shows the impedance locus for load flow in the forward direction ( $\delta$  equal to  $10$  degrees). In this case, the remote-end voltage  $V_R$  equals  $0.98$  pu. Regardless of the impedance loop measurement (ground fault loop or phase fault loop), the apparent impedance starts at a load value,  $Z_{LOAD}$ , that corresponds to  $R_f$  equals  $\infty$ . For active power flow in the

forward direction,  $Z_{LOAD}$  is on the right side (positive values of resistance) of the plane. As  $R_f$  starts decreasing, the apparent impedance describes the locus that Fig. 7 shows. Notice that with  $R_f$  equal to  $0$ , the apparent impedance is exactly equal to  $85$  percent of the line impedance.

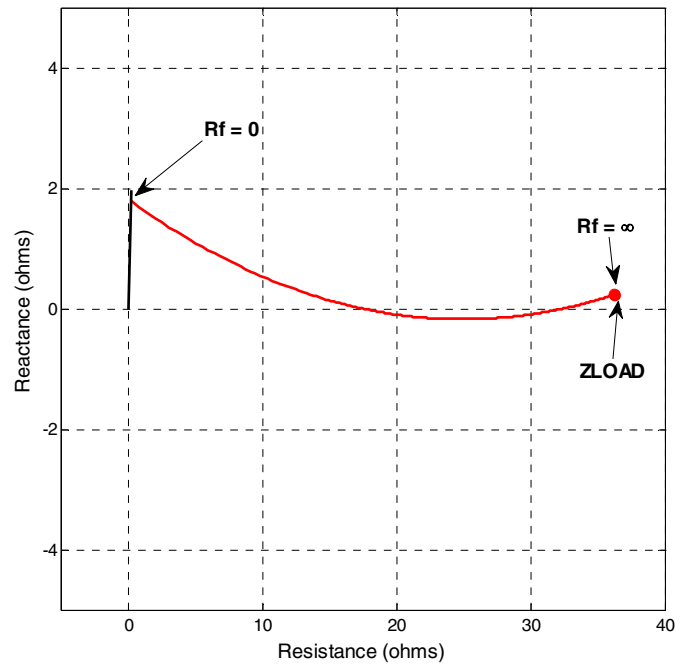


Fig. 7. Apparent impedance locus for load in the forward direction ( $\delta$  equal to  $10$  degrees)

Fig. 8 shows the impedance locus for incoming load flow ( $\delta$  equal to  $-10$  degrees). This apparent impedance makes it a challenge for the distance elements to detect large values of  $R_f$  and avoid element underreach.

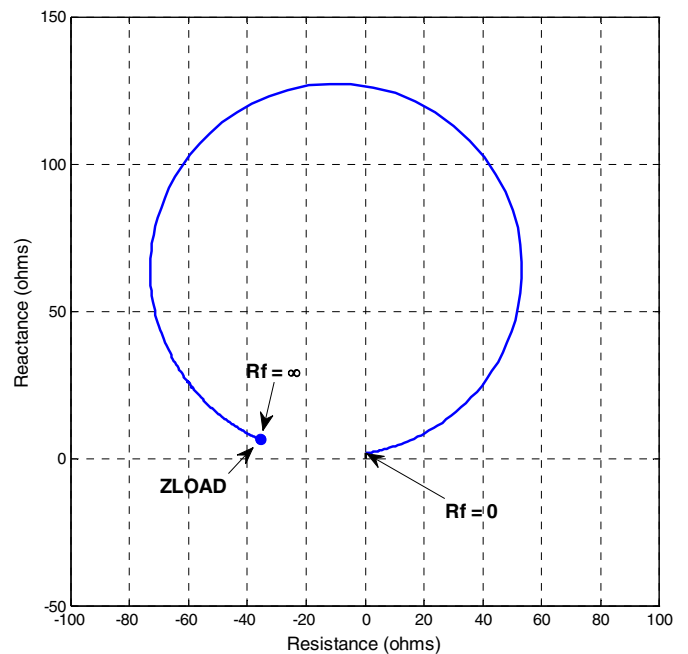


Fig. 8. Apparent impedance locus for incoming load flow ( $\delta$  equal to  $-10$  degrees)

## II. QUADRILATERAL DISTANCE ELEMENTS

Mho distance elements describe a natural and smooth curvature on the impedance plane. The shape is the result of a phase comparison of two quantities that yield the familiar circle on the apparent impedance plane [9]. Quadrilateral distance elements are not as straightforward. Combining distance elements has allowed designers to create all types of shapes and polygonal characteristics.

An impedance function with a quadrilateral characteristic requires the implementation of the following:

- A directional element
- A reactance element
- Two left and right blinder resistance calculations

Fig. 9 illustrates a typical quadrilateral element composed of three distance elements. The element that determines the impedance reach is the reactance element  $X$ . The element that determines the resistive coverage for faults is the right resistance element  $R_{right}$ . The element that limits the coverage for reverse flowing load is the left resistance element  $R_{left}$ . A directional check keeps the unit detecting faults in the forward direction only.

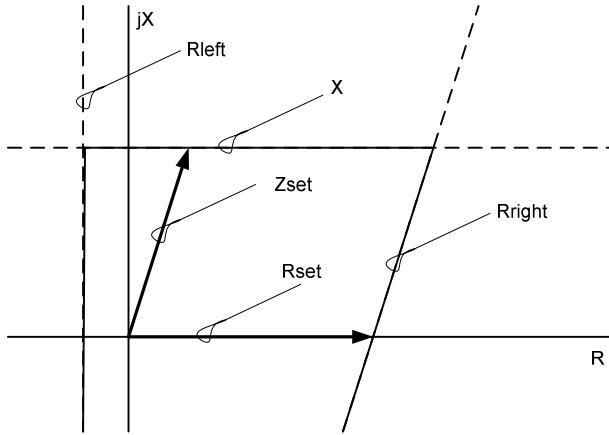


Fig. 9. Components of a quadrilateral distance element

The setting of the reach on the line impedance angle locus is denoted by  $Z_{set}$  in Fig. 9. It is not a setting on the  $X$  axis but is the reach on the line impedance. We will show that this setting is the pivot point of the line impedance reach. The  $R_{set}$  setting is the resistive offset from the origin. A line parallel to the line impedance is shown in Fig. 9.

The impedance lines in Fig. 9 are straight lines for practical purposes. The theory, however, shows that these lines are infinite radius circles [9]. The polarizing quantity for creating these large circles is the measured current at the relay location.

### A. Adaptive Reactance Element

Several protective relaying publications report that serious overreach problems are experienced by nonadaptive reactance elements because of forward load flow and  $R_f$  [1][2][11]. If the reactance element in a quadrilateral characteristic is not designed to accommodate the situation shown in Fig. 10, an

external fault with  $R_f$  may enter the operating area. The intrinsic curvature and beneficial shift of the mho circle are sufficient to overcome this problem. However, reactance lines need to be designed to accommodate this issue.

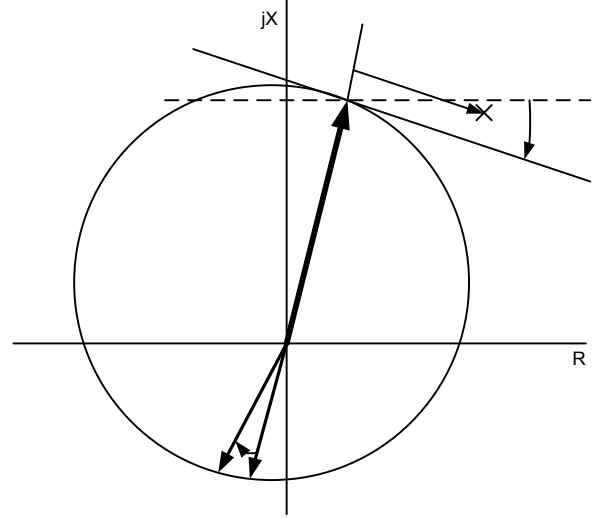


Fig. 10. The reactance and mho elements adapt to load conditions

Fig. 10 shows the desired behavior of the reactance line for forward load flow. A tilt in the shown direction is required. Several techniques have been proposed for this purpose, including a fixed characteristic tilt and the use of prefault load.

Interestingly, an infinite diameter mho circle provides the same tilt as a regular mho circle, and the reactive line becomes adaptive [9]. The proper polarizing current is the negative-sequence component [12]. The homogeneity of the negative-sequence network and the closer proximity of the  $I_2$  angle to the fault current ( $I_f$ ) angle makes the  $I_2$  current an ideal polarizing quantity.

To obtain the desired reactance characteristic for the AG loop, the following two quantities can be compared with a 90-degree phase comparator:

$$S1 = VRA - Z_{set}(IRA + k0 \cdot 3I0) \quad (2)$$

$$S2 = j(IR2)e^{jT} \quad (3)$$

Equations (4) and (5) define the resulting  $a$  and  $b$  vectors used to plot the reactance element characteristic [9].

$$a = Z_{set} \quad (4)$$

$$b = \infty e^{-j \left[ 90^\circ - T + \text{ang} \left( 1 + \frac{IA1}{IA2} + \frac{IA0}{IA2} \frac{Z_{set0}}{Z_{set}} \right) \right]} \quad (5)$$

$$k0 = \frac{Z_{set0} - Z_{set1}}{3 \cdot Z_{set1}} \quad (6)$$

where:

$k0$  is the zero-sequence compensating factor.

$Z_{set0}$  is the zero-sequence impedance reach derived from  $k0$  and  $Z_{set}$ .

Fig. 11 shows the adaptive behavior of the reactance line derived from (4) and (5). Calculating a proper homogeneity angle tilt (denoted by  $T$  in the equation), the unit ensures correct reach regardless of the direction of the load flow.

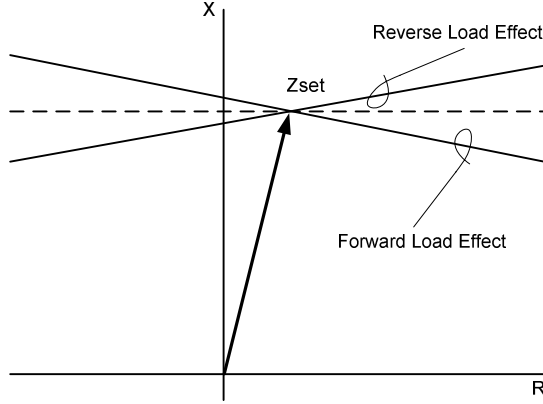


Fig. 11. Adaptive ground reactance element characteristic

For ground distance elements,  $I_0$  is another choice for polarizing the reactance element. This option is acceptable if the homogeneity factor,  $T$ , for the zero-sequence impedances is known.

For phase distance elements, using the negative-sequence current is also an option.

$$S1 = (VRB - VRC) - Zset(IRB - IRC) \quad (7)$$

$$S2 = j(IRB2 - IRC2)e^{iT} \quad (8)$$

The resulting  $a$  and  $b$  vectors are shown in (9) and (10).

$$a = Zset \quad (9)$$

$$b = \infty e^{-j\left(90 - T + \text{ang}\left(1 + \frac{IB1 - IC1}{IB2 - IC2}\right)\right)} \quad (10)$$

As described in [9], vector  $b$  defines the infinite diameter and the tilt angle, both of which are expressed in (5) for the ground reactance line and (10) for the phase reactance line. The resulting line is adaptive to the load flow direction, as shown in Fig. 11. The reactance line adapts properly to load flow and  $R_f$ .

### B. Adaptive Resistance Element

Fig. 9 shows that the right resistance element is responsible for the resistive coverage in a quadrilateral distance element. This component of the quadrilateral distance element should accommodate and detect as much  $R_f$  as possible.

In proposing an adaptive resistance line, it is possible to make the line static or adaptive as the reactance line. An adaptive resistive blinder is obtained by defining  $Rset$  in (2) and shifting (3) by  $(\theta L1 - 90^\circ)$ , where  $\theta L1$  is the angle of the positive-sequence line impedance. The benefit shown in Fig. 12 is a shift of the resistance element to the right, which accommodates faults with forward load flow. Equations (11) and (12) implement the adaptive ground resistance element.

$$S1 = VRA - Rset(IRA + k0 \cdot 3I0) \quad (11)$$

$$S2 = IR2 e^{j\theta L1} \quad (12)$$

Similarly, Equations (13) and (14) define the adaptive phase resistance element for phase faults.

$$S1 = (VRB - VRC) - Rset(IRB - IRC) \quad (13)$$

$$S2 = (IRB2 - IRC2) e^{j\theta L1} \quad (14)$$

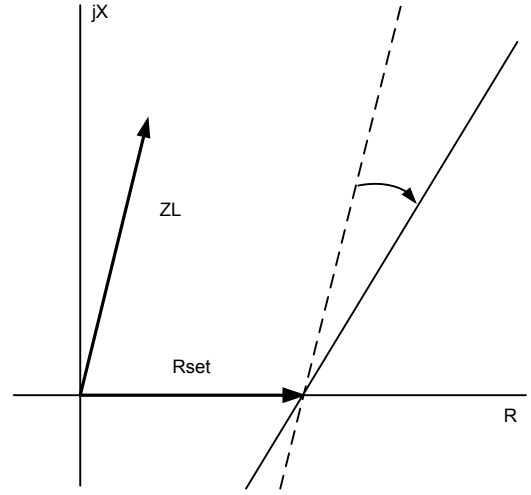


Fig. 12. Adaptive ground resistance element characteristic

While the use of negative-sequence current yields a beneficial tilt of the resistance element for load in the forward direction, as shown in Fig. 12, the tilt is in the opposite direction for load in the reverse direction. Therefore, the tilt is not beneficial under this condition.

Additional polarizing options, like that the alpha component ( $I1 + I2$ ) for ground and  $I1$  for phase distance elements, yield satisfactory tilt behavior for reverse load flow. The reverse load flow behavior is the same.

### C. Left Resistance Element

The left resistive line in Fig. 9 is responsible for limiting the operation of the quadrilateral element for reverse load flow. It does not need to be adaptive. Care has been taken not to include the origin to ensure satisfactory operation for very reactive lines.

### D. High-Speed Implementation

In many transmission line protection applications, subcycle operation is required for distance elements. In many relays, distance elements with mho or quadrilateral characteristics are available. When the distance elements selected have quadrilateral characteristics only, the same high-speed requirement is applicable for faults with low-resistance value.

In order to obtain subcycle operation with quadrilateral elements, the same dual-filter concept presented in [14] for mho elements is used here. The basic principle is to process the same distance function twice, using two types of voltage and current phasors: the function is processed first using half-cycle (high-speed) filter phasors and a second time with full-cycle (conventional) filter phasors. The final function state is obtained by the logical OR operation from the two processes.

For single-pole tripping applications, these three ground distance elements (AG, BG, and CG) need to be supervised with a faulted phase selection function.

For the purpose of implementing the directional element and the faulted phase selection for the high-speed part of the quadrilateral function, the algorithm described in [14] and [15] uses a function known as high-speed directional and fault type selection (HSD-FTS). It processes signals using half-cycle filters and superimposed quantities to provide the 14 directional signals listed in Table I.

TABLE I  
HIGH-SPEED DIRECTIONAL SIGNALS

Signal	Fault Description
HSD-AGF, HSD-AGR	Forward, reverse AG
HSD-BGF, HSD-BGR	Forward, reverse BG
HSD-CGF, HSD-CGR	Forward, reverse CG
HSD-ABF, HSD-ABR	Forward, reverse AB
HSD-BCF, HSD-BCR	Forward, reverse BC
HSD-CAF, HSD-CAR	Forward, reverse CA
HSD-ABCF, HSD-ABCR	Forward, reverse ABC

Because the HSD-FTS signals are derived from incremental currents and voltages, they will be available only for 2 cycles following the inception of a fault. Consequently, the high-speed quadrilateral signals are available for the same interval of time following the detection of a fault.

For the reactance element, the high-speed part of the quadrilateral characteristic implementation uses the same equations for the ground elements as the conventional counterpart uses with polarization based on negative- or zero-sequence current. During a pole open, the polarization by the sequence current (negative or zero) is replaced by the incremental impedance loop current so that the ground elements remain operational for single-pole tripping applications.

For the phase elements, polarization is based on the loop-impedance incremental current so that phase faults and single-pole tripping applications are automatically covered.

For the two resistance blinder calculations, the equations are identical to their conventional counterpart so that the steady-state resistance reach will be identical.

With the high-speed quadrilateral elements, reactance and resistance blinder calculations use a half-cycle filtering system to obtain fast operation.

The logic for an A-phase-to-ground fault is presented in Fig. 13. Similar logic is used for the two other ground fault elements and the phase elements.

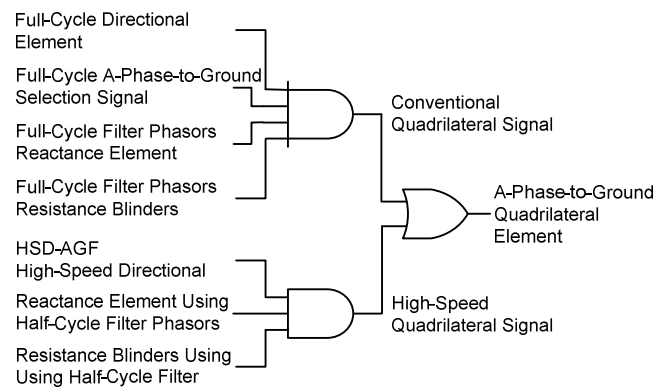


Fig. 13. High-speed quadrilateral characteristic logic for A-phase-to-ground faults

To illustrate the parallel operation of the high-speed and conventional quadrilateral elements, an A-phase-to-ground fault is staged at 33 percent of the line length of the high-voltage transmission line in the power network of Fig. 4. The impedance reach is set to 85 percent of  $Z_{L1}$ . The fault is staged at 100 milliseconds of the EMTP (Electromagnetic Transients Program) simulation.

Fig. 14 shows the distance to the fault calculations of the two reactance elements (high-speed and conventional) for  $R_f$  equal to 0 ohms. The high-speed element operates in 12.5 milliseconds, and the conventional element operates in 21 milliseconds.

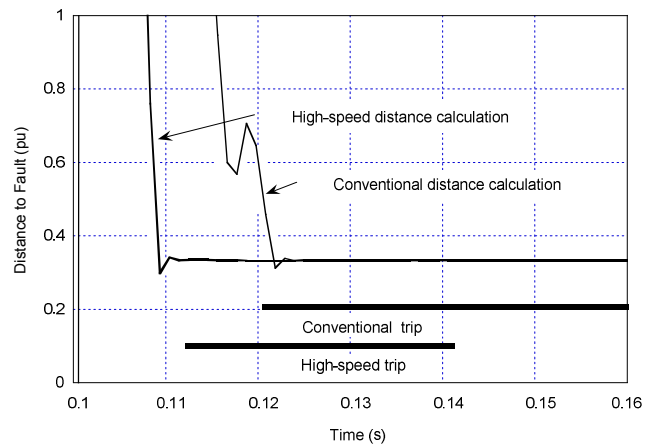


Fig. 14. High-speed and conventional distance element calculations for a 0-ohm, A-phase-to-ground fault at 33 percent of the line length

Fig. 15 depicts the same experiment but with a primary  $R_f$  equal to 50 ohms. The high-speed element has an operating time of 14.5 milliseconds, whereas the conventional element has an operating time of 25 milliseconds.

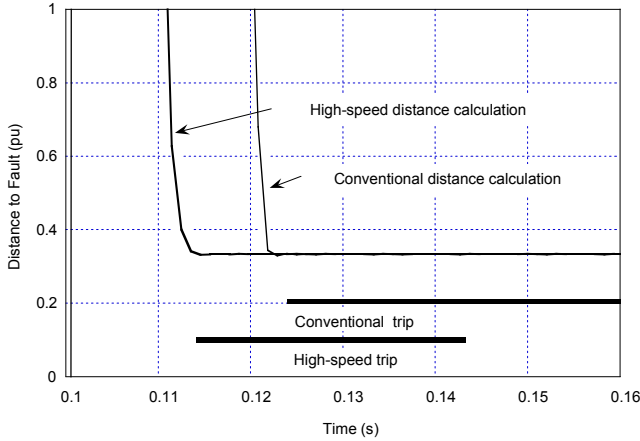


Fig. 15. High-speed and conventional distance element calculations for a 50-ohm, A-phase-to-ground fault at 33 percent of the line length

As a general rule, the quadrilateral high-speed logic will send an output signal a half cycle before the conventional logic. This corresponds most of the time to an overall subcycle operation for low  $R_f$  values. As illustrated in the two examples above, as  $R_f$  increases, both the fault current and the voltage dip will be reduced. Under these circumstances, the operation times of the high-speed and conventional quadrilateral elements will increase so that overall operation times close to or above 1 cycle will be more typical for high-resistance faults.

### III. QUADRILATERAL DISTANCE ELEMENT APPLICATION

#### A. Homogeneity Calculation

The reactive line in a quadrilateral distance element can be polarized with either negative-sequence ( $IR_2$ ) or zero-sequence ( $IR_0$ ) current to properly adapt to load flow, as shown in Fig. 11. Polarizing with these currents makes the line adaptive and less susceptible to overreach. A check is needed, however, to ensure effective Zone 1 quadrilateral ground and phase distance element behavior [13]. This check is for the homogeneity of the negative-sequence impedances (or zero-sequence impedances, if zero-sequence polarization has been used).

In a ground fault or asymmetrical phase fault, the total fault current always lags the source voltages. This fault current,  $IF$ , is the perfect polarizing current. It is in the same direction regardless of the type of fault (same angle but with different magnitude). Because the  $IF$  current is not measurable, the measured currents at the relay location are the only ones available. The negative-sequence current is an option for polarizing the reactance line of the quadrilateral element. The protective relay is measuring the local  $IR_2$  (negative-sequence current). The  $IF_2$  current is the proper current to use.

Fig. 16 illustrates the negative-sequence network of a simple transmission line and the respective source impedances at both terminals. If possible, this two-source network should be evaluated. If the system is slightly more complex (e.g., parallel lines), a short-circuit program can provide the  $IF_2$  and  $IR_2$  currents. The calculation should be done for a fault at the reach of the Zone 1, where  $m$  is approximately 80 percent.

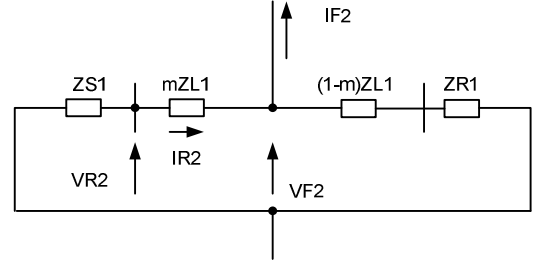


Fig. 16. Two-source negative-sequence network

The variable  $T$  is the homogeneity factor, and it is the angle difference between the fault current and the current measured at the relay location. Reference [12] illustrates the evaluation of this factor, which is the following current divider expression:

$$T = \arg\left(\frac{IF_2}{IR_2}\right) = \arg\left[\frac{ZS_1 + ZL_1 + ZR_1}{ZR_1 + (1-m)ZL_1}\right] \quad (15)$$

The angle  $T$  in (15) adjusts the measured  $IR_2$  current to the angle of the fault current  $IF_2$ . It is used in (3) and (8) to properly polarize the reactance line of the quadrilateral element.

When the ground quadrilateral element is polarized with zero-sequence current ( $IR_0$ ), use a similar expression to calculate  $T$  (15), except that the currents and impedances are zero sequence.

Equation (15) also provides some extra information regarding the homogeneity of the sequence network. For most transmission networks, the impedance angles in the negative-sequence network are very similar. Evaluating (15) yields a small angle, usually in the range of  $\pm 5$  degrees. On the other hand, in the zero-sequence network, the homogeneity angle varies considerably more.

In (3) and (8), the reactance line is effectively tilted by the  $T$  angle.

#### B. Load Encroachment

The quadrilateral distance elements discussed in this paper are inherently immune to load encroachment. The reactive line that defines the reach is polarized with negative-sequence currents, as shown in (3) and (8). The phase and ground reactive lines start their computation when there is a fault condition that implies an unbalance of ( $I_2/I_1$ ) or ( $I_0/I_1$ ) greater than the natural unbalance of the system, which is less than 10 percent.

In a full protection scheme, however, there should be provisions to detect three-phase faults. Although rare, this type of fault is possible. It usually is a fault with almost no  $R_f$ .

The three-phase fault detection element is obtained by using current self-polarization. For example, the BC loop would be polarized with:

$$S2 = j(IRB - IRC)e^{-jT} \quad (16)$$

To avoid overreach because of forward flowing load, the setting  $T$  in degrees is a tilt, most likely downward, for the reactive line. The resistive reach is polarized with positive-sequence current.

The three-phase quadrilateral element just described is set with the same reach as the phase-to-phase distance elements. It does require certain load considerations to avoid load encroachment.

If the transmission line is long and the resistive setting chosen conflicts with load, a load encroachment element is required. This element should clearly define the load area in the forward load flow direction. Fig. 17 illustrates a traditional and already widely used load-encroachment logic characteristic. The operating point of the load impedance in this region will clearly identify load conditions and prevent the three-phase fault detection algorithm from operating.

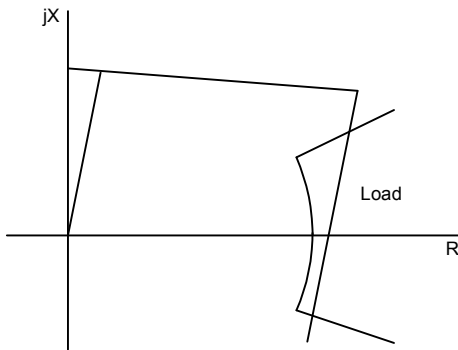


Fig. 17. Load encroachment for quadrilateral three-phase distance elements

### C. Out of Step

Much of the theory and discussion in literature on out-of-step detection can be applied to quadrilateral distance elements [16][17]. When power flows are oscillating in a power system, the apparent impedances measured by the distance elements describe a trajectory on the R-X plane. These oscillations can be caused by angular instability or simply switching lines in or out [17]. If the oscillations are contained within a maximum oscillation envelope and are damped over time, the power swings are considered stable. On the other hand, if the power swings are not damped over time, the power swings are said to be unstable.

On the R-X diagram shown in Fig. 18, a stable power swing impedance trajectory is contained on the right side (or the left side for reverse power flow) and eventually rests on a new load-impedance operating point. An unstable power swing, in contrast, will show a trajectory that crosses the plane from left to right (or right to left). Theoretically, and assuming the simple two-source network shown in Fig. 18, the unstable power swing will cross the electrical center of the system when the angle's difference between the two source voltages is close to 180 degrees apart. Unless the power system can be reduced to a two-source model, it is not a simple matter to

predict the impedance trajectory, and stability studies may be required.

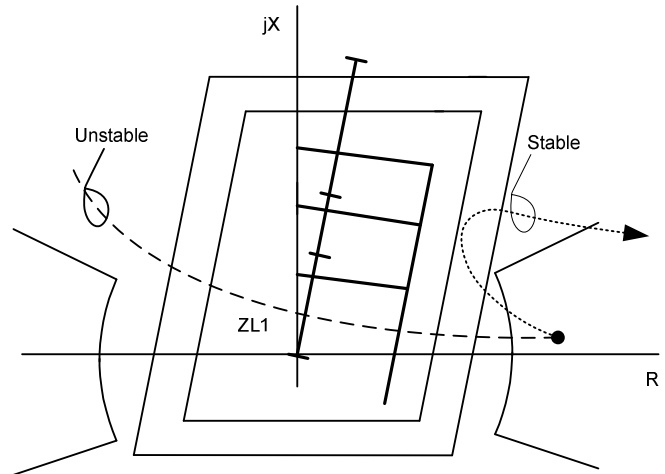


Fig. 18. Traditional dual-zone out-of-step characteristic

During power system oscillations, stability requirements demand that transmission lines remain in the power system. Tripping transmission lines unnecessarily jeopardizes the stability of the power system. It is therefore necessary to ensure that unstable trajectories on the R-X diagram entering distance element characteristics (shown in Fig. 18) do not unnecessarily trip the transmission line. However, some applications require tripping transmission lines in a controlled manner.

Out-of-step detection techniques traditionally take advantage of the slower speed of the apparent impedance trajectory on the R-X diagram for power swing conditions. The trajectory of the operating point changes from load to fault almost instantaneously for fault conditions.

Fig. 18 illustrates a traditional scheme comprised of two zones. If the inner zone operates after a set time delay (2 to 5 cycles), an out-of-step condition is detected. If the trajectory is due to a power system fault, both zones will operate within a short time window.

There are several philosophies to follow when setting the parameters of this scheme [17]. Some of the most important considerations are:

- The inner zone should not operate for stable swings. As shown in Fig. 18, a stable swing eventually returns to the load impedance.
- The outer zone should not include any possible load impedance. If load is included by the outer zone, there is a risk of incorrectly declaring a power swing condition.
- The distance from the inner to the outer zone on the impedance plane should be made as wide as possible to allow the detection of the power swing condition.
- The inner zone should not include any distance element zone that is to be blocked. For long line applications, achieving this goal for all distance zones may not be possible. We can place the inner zone across part of the distance element characteristic. This will effectively cut part of the characteristic.

Fig. 18 illustrates some of these considerations. Short lines present sufficient margin to accommodate the inner and outer zones together with any type of distance element, such as a quadrilateral distance unit, following the above guidelines. Long transmission lines, however, may not allow sufficient margin. Engineering judgment should be used to set the inner and outer zones, as well as the resistive reach of the quadrilateral element.

When determining the setting parameters, it may be very difficult to cover all possible scenarios of instability with a simple two-source model. Therefore, transient studies will be needed to understand the effectiveness of the scheme in Fig. 18.

Recently, a power swing detection algorithm was proposed that requires little information from the user [18]. This algorithm will detect and declare a power swing based on the estimation of the swing center voltage (SCV), which is the voltage at the electrical center of a two-source model. This voltage can be estimated with local measurements and its behavior used to detect an out-of-step condition. The advantage of this methodology is that no network information is required.

#### D. Series Capacitor Applications

It is common to apply directional comparison relaying systems in the protection of series-compensated transmission lines. Protective relays intended to protect these lines should be designed to accommodate the changing measured impedance (because of the MOVs [metal oxide varistors] and spark gaps in parallel with the capacitor bank) and subsynchronous voltages and currents that are characteristic of series capacitor-compensated systems [19]. Moreover, protective relaying systems located in adjacent lines should reliably determine the direction to a fault.

For distance elements that are polarized with voltage, like mho distance elements, the voltage inversion because of the series capacitor is properly handled with memory voltage [19][20]. Moreover, directional elements determine the correct direction to the fault [21].

Identifying the fault direction is important to keep the reactance and resistance lines of the quadrilateral distance element from operating improperly. An impedance-based negative-sequence polarized directional element (or an alternate zero-sequence polarized element for ground faults) will properly determine the direction to the fault, unless a current inversion is present. Depending on the location of the capacitor bank and the location of the voltage transformers (VTs), suggested settings for the directional thresholds (Z2F and Z2R) can be found in [20] and [21]. For the impedances of the compensated system in Fig. 19, the directional element threshold Z2F should be set to:

$$Z2F \leq \frac{(ZL1 - XC)}{2} \quad (17)$$

Setting this threshold as close to the origin as possible will ensure proper directional determination, unless a current reversal is possible in the power system.

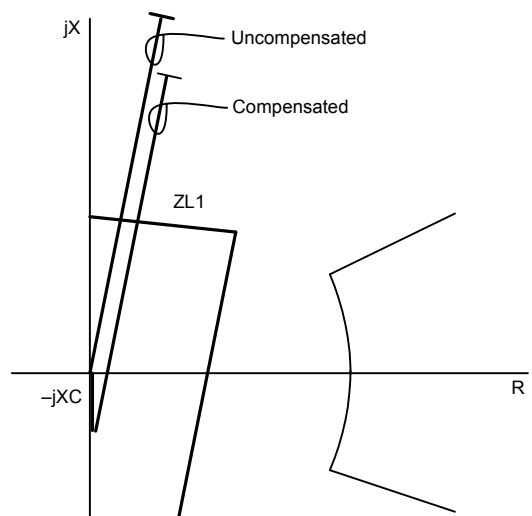


Fig. 19. Series capacitor applications

In Fig. 19, the perspective of a long line is shown. Series-compensated lines are long lines that require compensation to transfer more power. There are no short lines compensated with series capacitors. Also, in the vicinity of a series capacitor installation, subsynchronous oscillations of the voltages and currents are possible [19][20][21]. While the filtering in protective relays is very good at eliminating high-frequency components, the filtering is not efficient at eliminating lower frequencies. These subsynchronous transients, shown as impedance oscillations on the apparent impedance plane, eventually converge on the true apparent impedance, as illustrated in Fig. 20. This figure also shows that distance element overreach is a possibility.

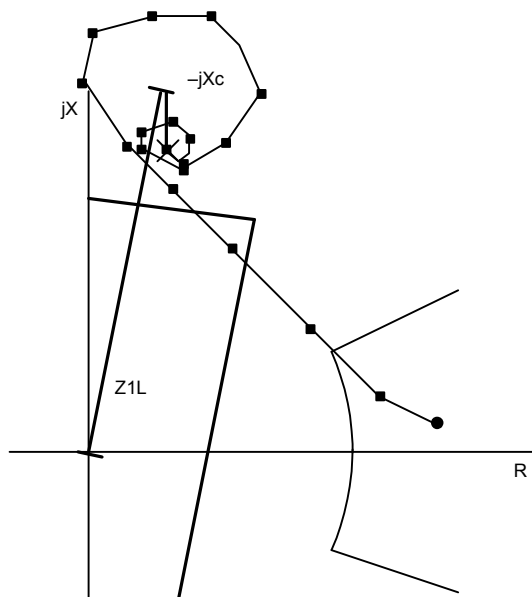


Fig. 20. Subharmonic frequency transients can cause distance elements to overreach

Zone 1 distance elements should account for the above phenomena by reducing the reach [20][21]. A good suggestion is to set the reach of the reactive line to half of the compensated line impedance [20]. On the other hand, protective relays can have an automatic reach adjustment based on a measured apparent impedance compared to a theoretically calculated value [14][21]. This way, the reach is automatically reduced to half of the compensated line impedance when transients are detected. The resistive reach should follow the recommendations for a long line (e.g.,  $R_{set}$  equal to one-half  $Z_{set}$ ).

The presence of the series capacitor in the power system modifies the homogeneity of the negative- and zero-sequence impedances. Therefore, when adjusting the homogeneity factor  $T$ , described in (18) and (19), the capacitor impedance should be considered. When using a negative-sequence current polarized reactance element:

$$T = \arg\left(\frac{IF2}{IR2}\right) = \arg\left[\frac{ZS1 + ZL1 - XC + ZR1}{ZR1 + (1-m)(ZL1 - XC)}\right] \quad (18)$$

And when using a zero-sequence polarized reactance line:

$$T = \arg\left(\frac{IF0}{IR0}\right) = \arg\left[\frac{ZS0 + ZL0 - XC + ZR0}{ZR0 + (1-m)(ZL0 - XC)}\right] \quad (19)$$

Notice that the zero- and negative-sequence impedance of a series capacitor are the same as the positive-sequence impedance.

Equation (18) for the uncompensated line should also be evaluated. The minimum calculated  $T$  value (most negative) should be used.

When applying any protective relaying scheme to series-compensated lines, transient simulation and testing are recommended [19][21]. This step ensures dependability and confirms proposed settings.

#### E. Single-Pole Trip Applications

In transmission line protection, it is common to use single-pole trip schemes. The scheme trips the faulted phase only for a single-line-to-ground fault. Once the pole is open, the other two phases are still conducting power, and the system is capable of remaining synchronized. During the open-pole interval, it is expected that the arc deionizes. After the open-pole interval, a reclosing command is sent to the breaker.

Current polarization with negative-sequence current (I2) or zero-sequence current (I0) is not reliable during the open-pole interval. The open pole makes the power system unbalanced, causing negative- and zero-sequence currents to flow. The consequence to distance elements polarized with sequence component currents, as in (3) and (8), is that the polarization becomes unreliable. Depending on the load flow direction, I2

and I0 will have different directions. Fortunately, there are other distance elements that will reliably operate during an open-pole condition [14]. The positive-sequence voltage-polarized mho element is stable during open-pole intervals and will reliably detect power system faults during this condition. In a practical scheme, the phase and ground quadrilateral elements should be disabled when an open-pole condition is detected. The high-speed quadrilateral distance element is implemented with incremental quantities and does not need to be disabled during the open-pole interval.

#### IV. SETTING THE QUADRILATERAL DISTANCE ELEMENT

Consider the A-phase-to-ground fault circuit of Fig. 4. Equation (20) determines the apparent impedance ( $Z_{app}$ ) that the relay installed at the left side of the line measures as a function of fault voltages and currents. Equation (21) determines  $Z_{app}$  as a function of  $R_f$  and fault location  $m$ .

$$Z_{app} = \frac{VA}{IA + k0 \cdot IR} \quad (20)$$

$$Z_{app} = m \cdot ZL1 + KR \cdot Rf \quad (21)$$

In (21),  $KR$  is a factor that depends upon the positive- and zero-sequence current distribution factors ( $C1$  and  $C0$ ) and is equal to:

$$KR = \frac{3}{2 \cdot C1 + C0(1 + 3 \cdot k0)} \quad (22)$$

$C1$  and  $C0$  are equal to:

$$C1 = \frac{(1-m) \cdot ZL1 + ZR1}{ZS1 + ZL1 + ZR1} \quad (23)$$

$$C0 = \frac{(1-m) \cdot ZL0 + ZR0}{ZS0 + ZL0 + ZR0} \quad (24)$$

$k0$  is the zero-sequence compensation factor equal to:

$$k0 = \frac{ZL0 - ZL1}{3 \cdot ZL1} \quad (25)$$

For no-load conditions ( $\delta$  equal to 0) and homogeneous systems, the resistive blinder of the adaptive quadrilateral element will assert for an  $R_f$  that satisfies this condition:

$$R_{app} < R_{set} \quad (26)$$

$$R_{app} = \text{Real}(KR) \cdot Rf \quad (27)$$

where  $R_{set}$  is the resistive reach setting. Alternatively, we can calculate  $R_{app}$  using relay voltage and currents for a fault at  $m$  according to (28).

$$R_{app} = \text{Real}(Z_{app}) - m \cdot \text{Real}(ZL1) \quad (28)$$

For the system in Fig. 4, Fig. 21 represents the values of  $Real(KR)$  as a function of  $m$  with a constant value of  $Rset$ . The increasing values of  $Real(KR)$  indicate that the maximum detectable  $Rf$  at no load decreases as the distance to the fault increases.

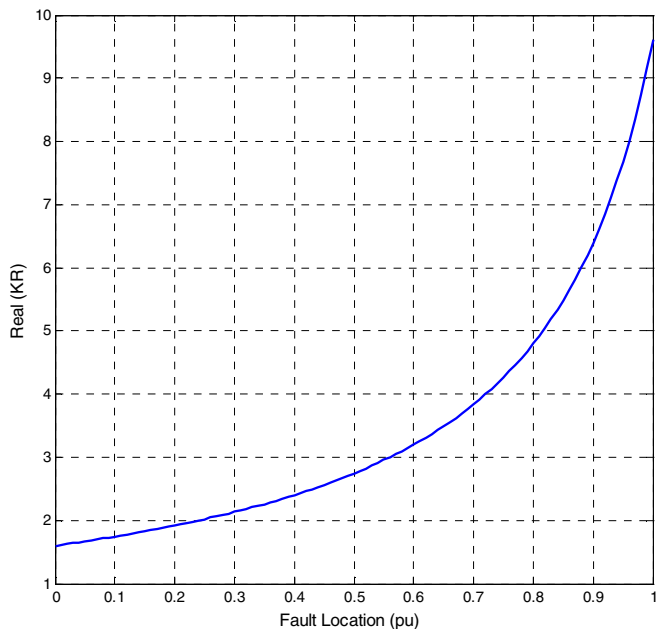


Fig. 21. Factor  $Real(KR)$  for the system of Fig. 4

Another consideration in determining the setting of the resistive coverage involves VT and CT (current transformer) errors. Reference [22] indicates that a composite angle error in the measurement  $\theta\epsilon$  can be assumed.

#### A. Zone 1

For a Zone 1 application, the requirement is that Zone 1 never overreaches for any fault at the end of the line. Assuming that for resistive faults at the end of the line there is an angle error  $\theta\epsilon$ , the effective path for increasing  $Rf$  will tilt down an extra  $\theta\epsilon$  degrees, as shown in Fig. 22. For increasing  $Rf$ , the intersection with the Zone 1 reactive line is the indication of the maximum  $Rset$  or  $Rmax$ . Using the law of sines and trigonometry,  $Rmax$  can be expressed as:

$$Rmax = \frac{\sin(\theta\epsilon + \theta L1)}{\sin(\theta\epsilon)} \cdot (1 - Zset\_pu) \cdot |ZL1| \quad (29)$$

Equation (29) defines  $Rmax$ , the maximum secure resistive reach setting for Zone 1, taking into account CT, VT, relay measurement errors, and  $\theta\epsilon$ .  $Rmax$  is a function of the impedance reach setting  $Zset$ , the positive-sequence line impedance magnitude  $|ZL1|$  and angle  $\theta L1$ , and the total angular error in radians  $\theta\epsilon$  [22].

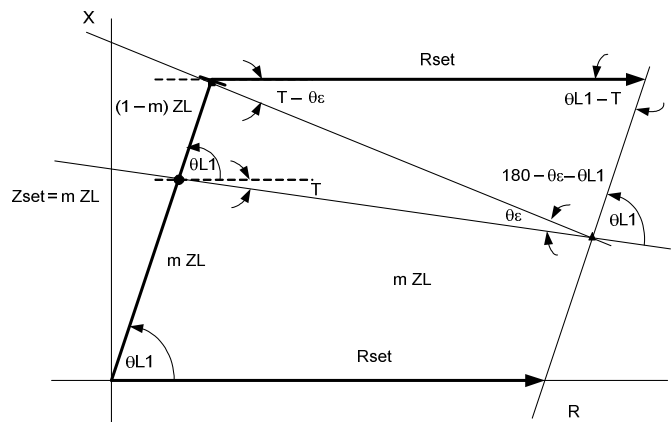


Fig. 22. CT and VT error evaluation for Zone 1

Fig. 23 shows the  $Rmax$  pu as a function of  $Zset$  for  $\theta L1$  equal to 40, 55, 70, and 75 degrees and  $\theta\epsilon$  equal to 2 degrees.

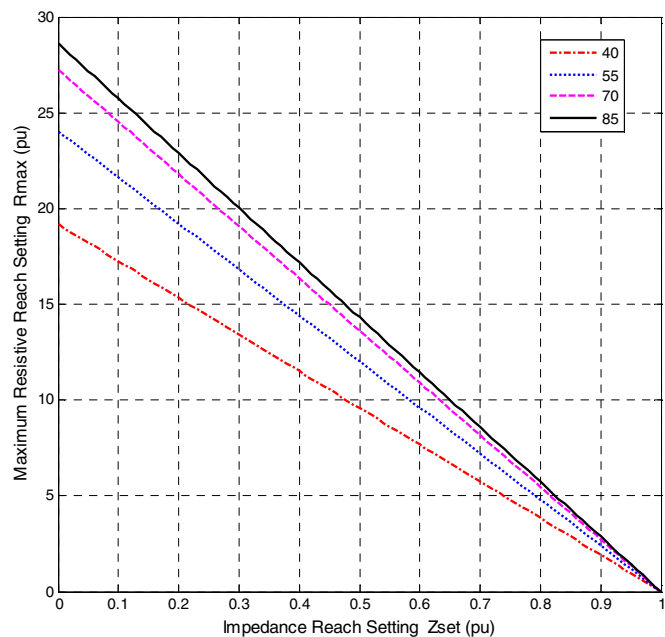


Fig. 23. Maximum resistive reach setting as a function of the impedance reach due to measurement errors

A typical Zone 1 impedance reach setting for short lines is 70 percent. For the system in Fig. 4,  $Zset\_zone1$  is equal to 1.4 ohms secondary.

With  $Zset$ ,  $|ZL1|$ ,  $\theta L1$ , and  $\theta\epsilon$ , we can calculate  $Rmax$  using (29) or obtain the pu value  $Rmax\_pu$  with respect to the total positive-sequence line impedance from Fig. 23. In this case,  $Rmax$  equals 17.17 ohms secondary, or  $Rmax\_pu$  equals 8.58 pu.

Additionally, we need to verify that the fault current is above the maximum relay sensitivity. In this case, the residual current is 3.0 A secondary, and the relay sensitivity is 0.25 A. Therefore, the relay can see the fault at 70 percent of the line with  $Rf$  equal to 25 ohms primary.

Fig. 24 shows the apparent resistance for different  $R_f$  values for a fault at 70 percent of the line. Note that with  $R_{set\_zone1}$  equal to 11.52 ohms, the quadrilateral element can see 3 ohms secondary or 25 ohms primary.

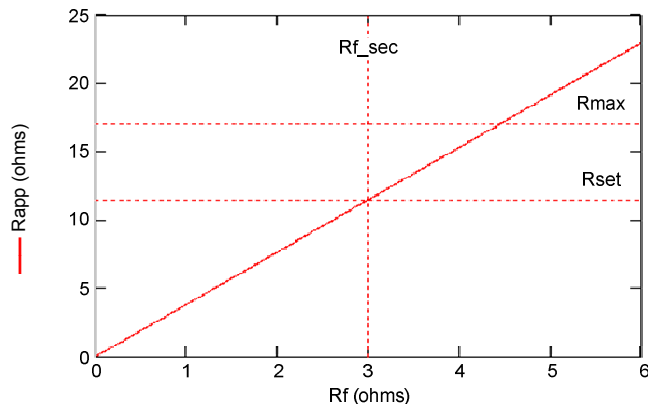


Fig. 24. Apparent resistance for a fault at 70 percent of the line

Fig. 25 shows the margin of the selected  $R_{set}$  with respect to  $R_{max}$  for the selected  $Z_{set}$ .

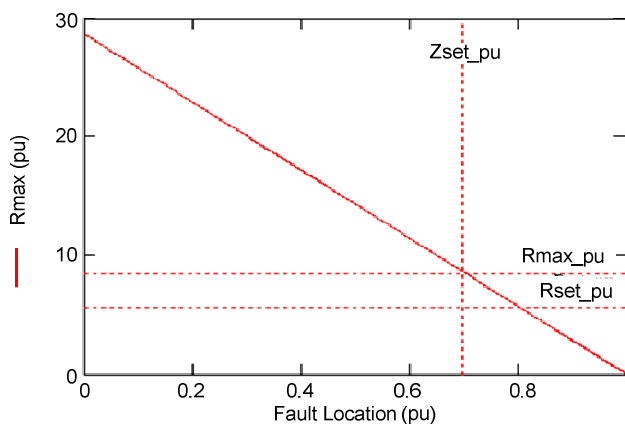


Fig. 25. Margin of  $R_{set}$  at  $Z_{set\_zone1}$  equal to 0.7 pu

Fig. 26 shows that the quadrilateral distance element can see up to 3 ohms for faults at 70 percent of the line for  $R_{set}$  equal to 11.52 ohms.

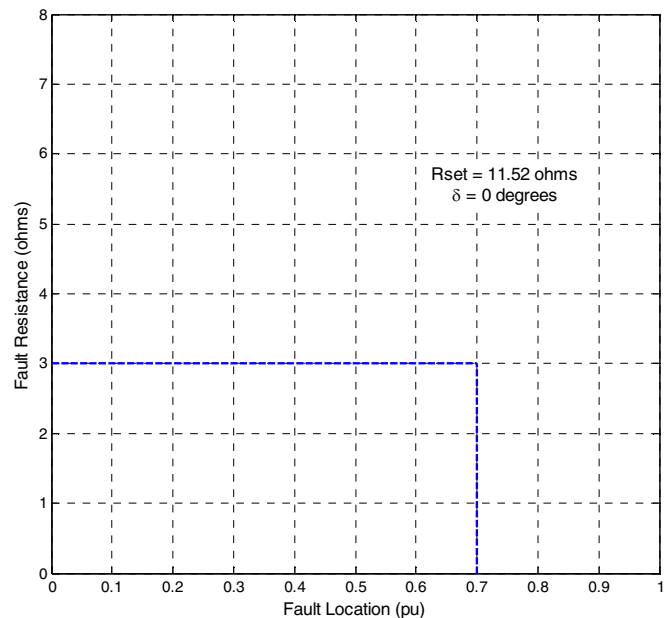


Fig. 26. Maximum  $R_f$  coverage with  $R_{set}$  equal to 11.5 ohms for faults along the line

The analysis carried out for a phase-to-ground fault can also be applied for phase-to-phase faults. In these cases, the factor  $KR$  is equal to:

$$KR = \frac{1}{2 \cdot CI} \quad (30)$$

For no-load conditions ( $\delta$  equal to 0) and homogeneous systems, the resistive blinder of the phase quadrilateral element will assert for an  $R_f$  that satisfies (31) or (32).

$$\frac{R_f}{2 \cdot \text{Real}(CI)} < R_{set} \quad (31)$$

$$R_{app} = \text{Real}\left(\frac{V\phi\phi}{I\phi\phi}\right) - m \cdot \text{Real}(ZL1) \quad (32)$$

### B. Zone 2

When considering overreaching zones, it is important to determine the maximum underreach and verify that the zone covers at least the expected  $R_f$ . For example, in a Zone 2 application, it is expected that all faults on the line and those at the remote terminal will be detected. It is a common practice to set the Zone 2 reach to 120 percent of the line length. However, in certain circumstances, this impedance reach would not guarantee coverage for faults with  $R_f$ , and a longer reach would be required.

Following is a conservative approach to set Zone 2 that guarantees that the overreaching element sees all faults with specific  $R_f$  coverage. Fig. 27 shows the apparent resistance for a homogeneous system and no-load conditions.

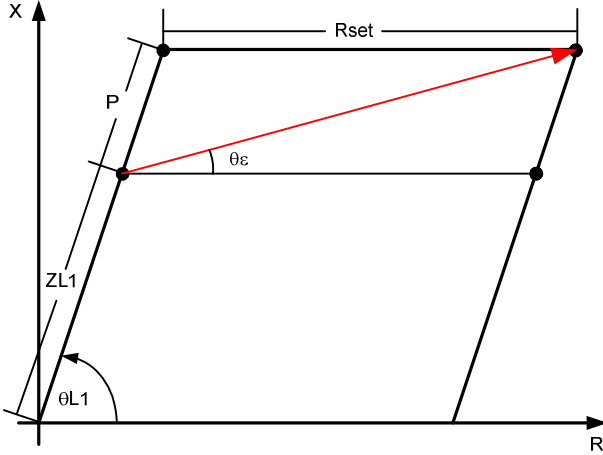


Fig. 27. Apparent impedance for an end-of-line fault considering measurement errors

From Fig. 27, we can estimate the required resistive reach  $Rset\_zone2$  and impedance reach  $Zset\_zone2$  settings according to (33) and (34) for a desired  $R_f$  coverage.

$$Rset\_zone2 = \frac{\sin(\theta_{L1} + \theta_{\epsilon})}{\sin(\theta_{L1})} \cdot \text{Real}(KR) \cdot R_f \cdot |e^{-j\theta_{\epsilon}}| \quad (33)$$

$$Zset\_zone2 = |ZL1| - \frac{\sin(\theta_{\epsilon})}{\sin(\theta_{L1} + \theta_{\epsilon})} \cdot Rset\_zone2 \quad (34)$$

We can represent  $Rset\_zone2\_pu$  as a function of  $Ppu$  according to (35). These values are the normalized values of  $Rset\_zone2$  and  $P$  (see Fig. 27) with respect to  $|ZL1|$ .

$$Rset\_zone2\_pu = -\frac{\sin(\theta_{L1} + \theta_{\epsilon})}{\sin(\theta_{\epsilon})} \cdot Ppu \quad (35)$$

Fig. 28 shows  $Rset\_zone2\_pu$  for  $\theta_{L1}$  equal to 40, 55, 70, and 85 degrees and for  $\theta_{\epsilon}$  equal to  $-2$  degrees.

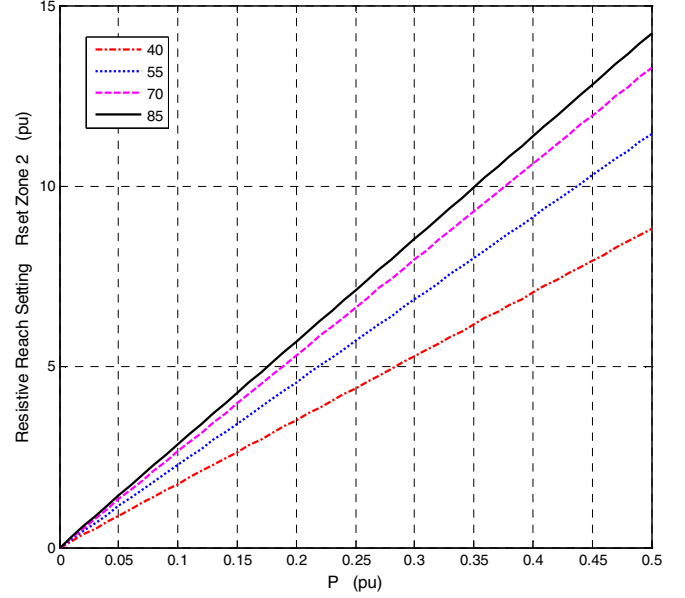


Fig. 28. The resistive reach setting as a function of the impedance reach setting for several values of  $\theta_{L1}$

For the relay in Fig. 4, we calculate  $Rset\_zone2$  for a desired  $R_f$  equal to 3 ohms secondary. Using (33) with  $\theta_{\epsilon}$  equal to  $-2$  degrees and a fault at the end of the line, we obtain  $Rset\_zone2$  equal to 28.69 ohms secondary and  $Rset\_zone2\_pu$  equal to 14.35 pu. From Fig. 28, we obtain the required value of  $Ppu$  and the Zone 2 impedance reach  $Zset\_zone2\_pu$  equal to 1.5 or 150 percent of  $|ZL1|$ .

## V. DISTANCE ELEMENT PERFORMANCE

### A. Traditional Distance Element Characteristics

Adaptive quadrilateral phase and ground distance elements were designed to improve  $R_f$  coverage in short line applications. A previous distance relay included a ground quadrilateral distance element characteristic with an adaptive reactance element and two resistance elements that calculate  $R_f$  according to (36) and a ground mho distance characteristic with an adaptive mho element that calculates the distance to the fault according to (37) [12]

$$R\ relay1 = \frac{\text{Im}\left[V \cdot (I \cdot e^{j\theta_{L1}})^*\right]}{\text{Im}\left[\frac{3}{2} \cdot (I2 + I0) \cdot (I \cdot e^{j\theta_{L1}})^*\right]} \quad (36)$$

$$m\ relay1 = \frac{\text{Re}\left[V \cdot (V1\_mem)^*\right]}{\text{Re}\left[I \cdot e^{j\theta_{L1}} \cdot (V1\_mem)^*\right]} \quad (37)$$

### B. Adaptive Resistance Element

Fig. 29 shows the quadrilateral distance element characteristic that uses the adaptive reactance element of the previous design with an adaptive resistive element.

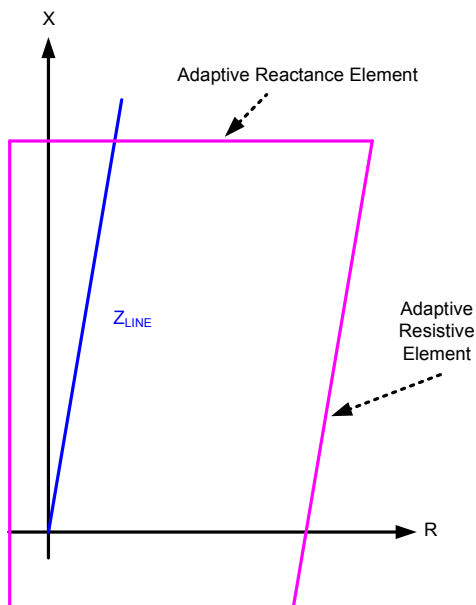


Fig. 29. Quadrilateral distance element characteristic with adaptive resistance element

The adaptive resistive element calculates  $R_f$  according to (38) and (39), and compares the minimum of the two calculation results against the resistive setting.

$$R_2 = \frac{\text{Im} \left[ V \cdot (I_2 \cdot e^{j\theta_{L1}})^* \right]}{\text{Im} \left[ I \cdot (I_2 \cdot e^{j\theta_{L1}})^* \right]} \quad (38)$$

$$R_\alpha = \frac{\text{Im} \left[ V \cdot (I_\alpha \cdot e^{j\theta_{L1}})^* \right]}{\text{Im} \left[ I \cdot (I_\alpha \cdot e^{j\theta_{L1}})^* \right]} \quad (39)$$

Equation (38) is equivalent to (11) and (12). It uses a different form of phase comparator equation. Equation (39) uses the alpha component ( $I_\alpha = I_1 + I_2$ ).

### C. Resistive Coverage

To compare the resistive coverage of the traditional distance elements with the adaptive resistive element, we use the system in Fig. 4 and perform the tests discussed in the following sections.

#### 1) Faults at Multiple Locations

We calculate the maximum  $R_f$  that the distance elements can detect for an A-phase-to-ground fault for  $m$  values from 0 to 1 and load angles of  $\delta$  equal to  $-10$ ,  $0$ , and  $10$  degrees. The quadrilateral distance elements have a resistive reach ( $R_{set}$ )

setting of 11.52 ohms and an impedance reach ( $Z_{set}$ ) setting of 120 percent of  $Z_{L1}$ . The mho distance element has a reach of 120 percent of  $Z_{L1}$ . The sensitivity of all the distance elements is  $0.05 \cdot I_{nom}$ .

Fig. 30, Fig. 31, and Fig. 32 show the  $R_f$  coverage of mho and quadrilateral distance elements. We observe that the  $R_f$  coverage is severely reduced as the fault approaches the end of the line. As expected, the mho element is the one with less  $R_f$  coverage, and the adaptive resistance element has the greatest  $R_f$  coverage, especially for power flow in the forward direction,  $\delta$  equal to 10 degrees.

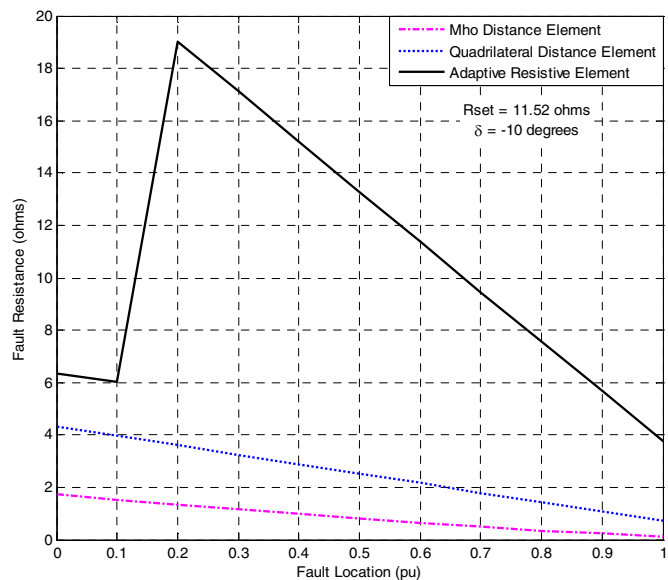


Fig. 30.  $R_f$  coverage of mho and quadrilateral distance elements for  $\delta$  equal to  $-10$  degrees

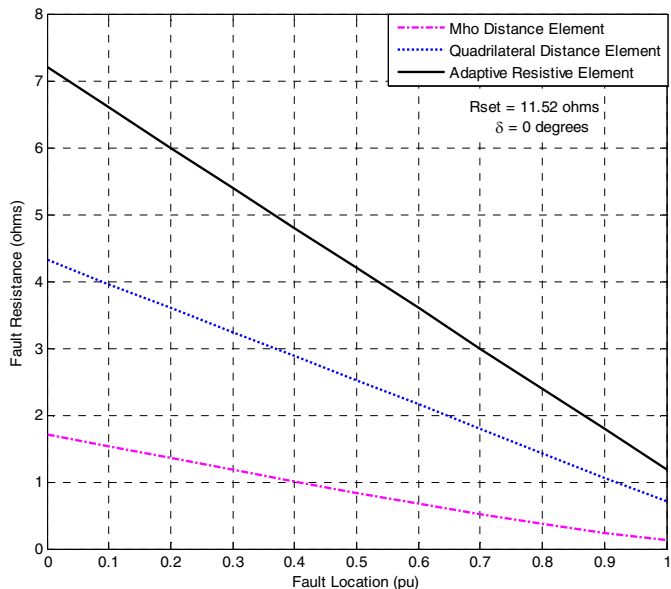


Fig. 31.  $R_f$  coverage of mho and quadrilateral distance elements for  $\delta$  equal to 0 degrees

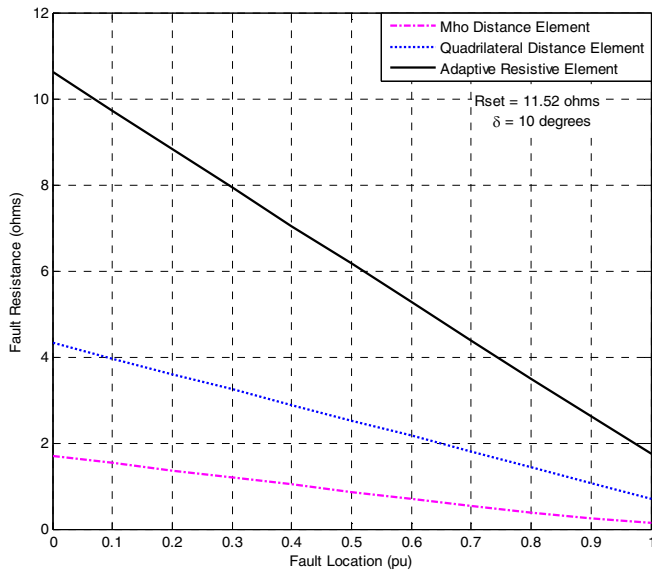


Fig. 32.  $R_f$  coverage of mho and quadrilateral distance elements for  $\delta$  equal to 10 degrees

2) Faults at  $m$  Equal to 0.7 for Multiple Load Angles

We calculate the  $R_f$  coverage for a fault at 70 percent of the line and different load angles (see Fig. 33). The adaptive resistance element has the highest  $R_f$  coverage, while the mho element has the lowest  $R_f$  coverage.

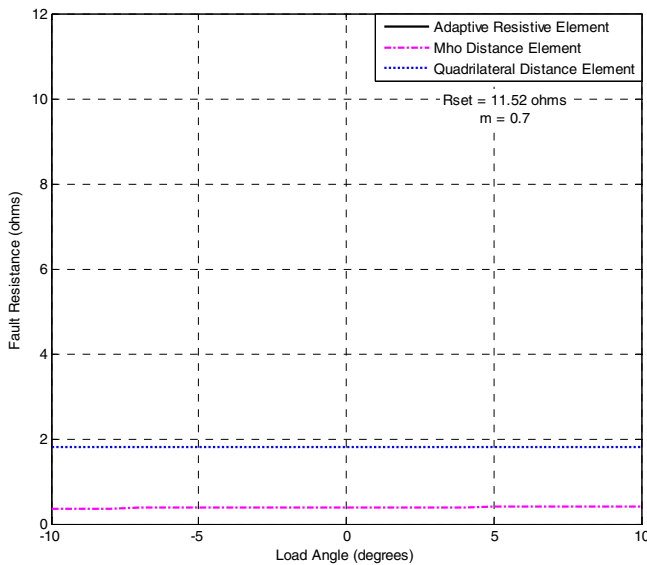


Fig. 33.  $R_f$  coverage for faults at 70 percent of the line with different load angles

D. Adaptive Behavior

A carefully designed quadrilateral characteristic should have an adaptive reactance line to avoid overreach because of load in the forward direction and  $R_f$ . Moreover, this paper has presented the concept of an adaptive resistive line that beneficially tilts to detect more  $R_f$ .

Two figures will be used to illustrate the adaptive behavior of the reactive line. Fig. 34 illustrates a ground fault detected from the terminal with forward load flow. Fig. 35 shows the same fault, with the same  $R_f$ , detected from the other terminal (i.e., the terminal with reverse direction load flow).

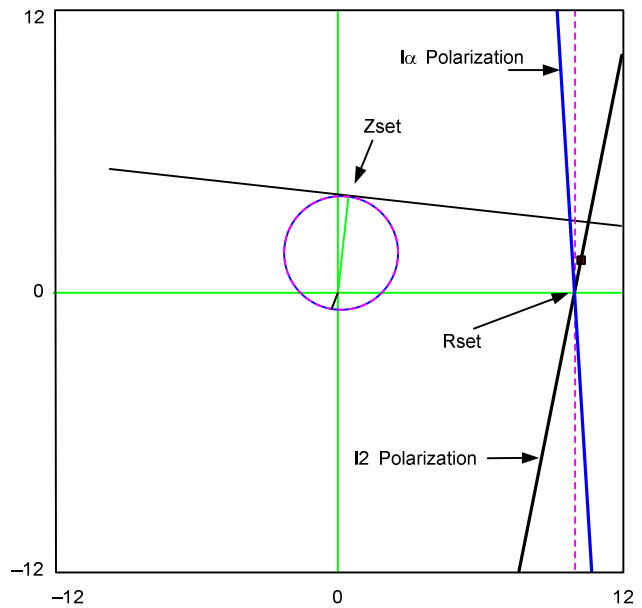


Fig. 34. Example of a ground fault detected from the forward load flow direction terminal

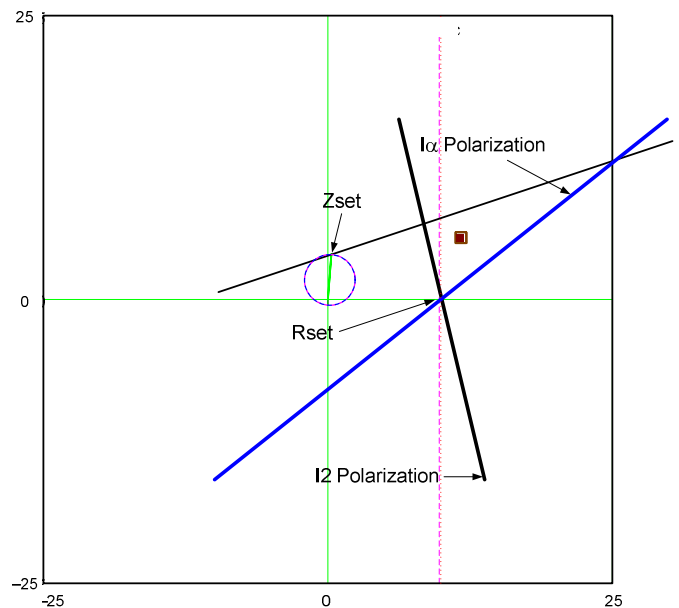


Fig. 35. Example of a ground fault detected from the reverse load flow direction terminal

Fig. 34 and Fig. 35 illustrate the adaptive behavior of the quadrilateral distance element. Because these figures are for illustrative purposes, the power system impedances, fault location, and/or  $Rf$  value are not relevant to the discussion. These two figures simply illustrate the adaptive behavior of the reactance and resistive lines.

The fault type is a ground fault; and the ground quadrilateral element is formed with a reactance line polarized with negative-sequence current (the preferred polarization). The two resistance elements are polarized with negative sequence (I2) and with the alpha component (I1 + I2). The polarization is what makes the lines adaptive, as explained in the previous sections.

Fig. 34 and Fig. 35 provide a wealth of information about the behavior of these impedance lines, including the following:

- The reactance element pivots on the line impedance reach, and that point is fixed. The resistance elements pivot on the resistive reach, which is a setting.
- The degree at which these lines tilt is determined by the power system parameters and operating conditions. These include line impedances, load flow, and  $Rf$ .
- The mho circle and reactance line tilt at the same time and in the same direction.
- The resistance element trip decision is the OR combination of either resistive line. Their behavior is dependent on the direction of the load flow, and their operation is complementary to each other.

For the forward load flow terminal in Fig. 34, we conclude:

- The reactance element tilts beneficially in a clockwise direction. This behavior prevents overreaching because of high-resistance load flow.
- The resistance element polarized with negative-sequence current will adapt to provide better resistive reach coverage. This resistive line will make the decision for faults with load in the forward direction.
- The resistance element polarized with the alpha component current tilts in the opposite direction. The resistive coverage of this characteristic is less effective compared to the other resistive line.

For the reverse load flow terminal in Fig. 35, we conclude:

- The reactance element moves in the direction that the apparent impedance locus moves, as shown in Fig. 10.
- The resistance element polarized with negative-sequence current moves in the opposite direction and with less resistive coverage.
- The resistance element polarized with the alpha component provides more effective coverage and will detect the fault.

## VI. CONCLUSIONS

Power system faults present different values of  $Rf$ . Ground faults present a larger value of  $Rf$  because of the arc resistance and tower footing resistance.

Short line protection applications with distance elements favor the use of quadrilateral distance elements for phase and ground fault protection. The expected  $Rf$  for short lines can be in the same order of magnitude as the impedance of the transmission line.

$Rf$  and power flow have the effect of modifying the apparent impedance measured by the distance element. The description of the  $Rf$  influence was plotted for different  $Rf$  values and load flows.

Especially for short lines, quadrilateral distance elements can detect faults with higher  $Rf$  than mho distance elements. Instrument transformers and relay measurement errors limit the  $Rf$  coverage in short line applications.

An adaptive characteristic for ground and phase quadrilateral distance elements was presented. The reactance element, polarized with negative-sequence current, adapts based on the direction of the load flow and prevents overreaching issues associated with load flow in the forward direction. Resistance elements are polarized with two quantities simultaneously. The negative-sequence polarization has a better  $Rf$  coverage for forward load flow. Using ground distance (alpha component) and phase distance (positive-sequence component) provides better coverage for faults with reverse load flow. For the resistance elements, running two polarizations at the same time helps to detect as much  $Rf$  as possible.

A high-speed version of the quadrilateral elements typically improves the speed of operation by half a cycle. These elements are required in applications where high-speed tripping times are required. These elements provide subcycle operating speeds and operate reliably during open-pole conditions.

The paper presented an improved distance element with an adaptive quadrilateral characteristic that can be part of a line protection relay.

The performance of the adaptive quadrilateral distance element was compared to a previous quadrilateral implementation, showing the benefits. A graphical illustration of the performance expected from the reactance and resistive lines was presented with an example in Fig. 34 and Fig. 35.

The  $Rf$  coverage of the adaptive quadrilateral element increases for terminals with forward direction load flow.

The phase quadrilateral distance elements presented in this paper are suitable for any transmission line application, but because of their nature, they fit better in short line applications. No distance element, however, can provide better sensitivity and  $Rf$  coverage than directional overcurrent elements in a pilot scheme.

## VII. REFERENCES

- [1] S. Ward, "Comparison of Quadrilateral and Mho Distance Characteristic," proceedings of the 26th Annual Western Protective Relay Conference, Spokane, WA, October 1999.
- [2] J. Holbach, V. Vadlamani, and Y. Lu, "Issues and Solutions in Setting a Quadrilateral Distance Characteristic," proceedings of the 61st Annual Conference for Protective Relay Engineers, College Station, TX, April 2008.
- [3] J. Mooney and J. Peer, "Application Guidelines for Ground Fault Protection," proceedings of the 24th Annual Western Protective Relay Conference, Spokane, WA, October 1997.
- [4] S. Sebo, "Zero-Sequence Current Distribution Along Transmission Lines," IEEE Transactions on Apparatus and Systems, PAS-88, Issue 6, June 1969.
- [5] G. Swift, D. Fedirchuk, and T. Ernst, "Arcing Fault 'Resistance' (It Isn't)," proceedings of the Georgia Tech Fault and Disturbance Analysis Conference, Atlanta, GA, May 2003.
- [6] H. Khodr, A. Menacho e Moura, and V. Miranda, "Optimal Design of Grounding System in Transmission Line," proceedings of the International Conference on Intelligent Systems Applications to Power Systems, November 2007.
- [7] V. Terzija and H. Koglin, "New Approach to Arc Resistance Calculation," IEEE PES Winter Meeting, Vol. 2, 2001.
- [8] L. Popovic, "A Digital Fault-Location Algorithm Taking Into Account the Imaginary Part of the Grounding Impedance at the Fault Place," IEEE Transactions on Power Delivery, Vol. 18, Issue 4, October 2003.
- [9] F. Calero, "Distance Elements: Linking Theory With Testing," proceedings of the 35th Annual Western Protective Relay Conference, Spokane, WA, October 2008.
- [10] J. Roberts, E. O. Schweitzer, III, R. Arora, and E. Poggi, "Limits to the Sensitivity of Ground Directional and Distance Protection," proceedings of the 1997 Spring Meeting of the Pennsylvania Electric Association Relay Committee, Allentown, PA, May 1997.
- [11] J. Roberts, A. Guzmán, and E. O. Schweitzer, III, "Z = V/I Does Not Make a Distance Relay," proceedings of the 20th Annual Western Protective Relay Conference, Spokane, WA, October 1993.
- [12] E. O. Schweitzer, III and J. Roberts, "Distance Relay Element Design," proceedings of the 46th Annual Conference for Protective Relay Engineers, College Station, TX, April 1993.
- [13] *SEL-421 Instruction Manual*. Available: <http://www.selinc.com>.
- [14] A. Guzmán, J. Mooney, G. Benmouyal, and N. Fischer, "Transmission Line Protection System for Increasing Power System Requirements," proceedings of the 55th Annual Conference for Protective Relay Engineers, College Station, TX, April 2002.
- [15] G. Benmouyal and J. Roberts, "Superimposed Quantities: Their True Nature and Application in Relays," proceedings of the 26th Annual Western Protective Relay Conference, Spokane, WA, October 1999.
- [16] D. Tziouvaras and D. Hou, "Out-of-Step Protection Fundamentals and Advancements," proceedings of the 30th Annual Western Protective Relay Conference, Spokane, WA, October 2003.
- [17] J. Mooney and N. Fischer, "Application Guidelines for Power Swing Detection on Transmission Systems," proceedings of the 32nd Annual Western Protective Relay Conference, Spokane, WA, October 2005.
- [18] G. Benmouyal, D. Tziouvaras, and D. Hou, "Zero-Setting Power-Swing Blocking Protection," proceedings of the 31st Annual Western Protective Relay Conference, Spokane, WA, October 2004.
- [19] H. Altuve, J. Mooney, and G. Alexander, "Advances in Series-Compensated Line Protection," proceedings of the 35th Annual Western Protective Relay Conference, Spokane, WA, October 2008.
- [20] J. Mooney and G. Alexander, "Applying the SEL-321 Relay on Series-Compensated Systems," SEL Application Guide AG2000-11. Available: <http://www.selinc.com>.
- [21] F. Plumtre, M. Nagpal, X. Chen, and M. Thompson, "Protection of EHV Transmission Lines With Series Compensation: BC Hydro's Lessons Learned," proceedings of the 62nd Annual Conference for Protective Relay Engineers, College Station, TX, March 2009.
- [22] E. O. Schweitzer, III, K. Behrendt, and T. Lee, "Digital Communications for Power System Protection: Security, Availability and Speed," proceedings of the 25th Annual Western Protective Relay Conference, Spokane, WA, October 1998.

## VIII. BIOGRAPHIES

**Fernando Calero** received his BSEE in 1986 from the University of Kansas, his MSEE in 1987 from the University of Illinois (Urbana-Champaign), and his MSEPE in 1989 from the Rensselaer Polytechnic Institute. From 1990 to 1996, he worked in Coral Springs, Florida, for the ABB relay division in the support, training, testing, and design of protective relays. Between 1997 and 2000, he worked for Itec Engineering, Florida Power and Light, and Siemens. Since 2000, Fernando has been an application engineer in international sales and marketing for Schweitzer Engineering Laboratories, Inc., providing training and technical assistance.

**Armando Guzmán** received his BSEE with honors from Guadalajara Autonomous University (UAG), Mexico. He received a diploma in fiber-optics engineering from Monterrey Institute of Technology and Advanced Studies (ITESM), Mexico, and his MSEE from the University of Idaho, USA. He lectured at UAG and University of Idaho in power system protection and power system stability. Since 1993, Armando has been with Schweitzer Engineering Laboratories, Inc. in Pullman, Washington, where he is research engineering manager. He holds several patents in power system protection and metering. He is a senior member of IEEE.

**Gabriel Benmouyal, P.E.** received his BAsC in Electrical Engineering and his MASc in Control Engineering from Ecole Polytechnique, Université de Montréal, Canada, in 1968 and 1970. In 1969, he joined Hydro-Québec as an instrumentation and control specialist. He worked on different projects in the fields of substation control systems and dispatching centers. In 1978, he joined IREQ, where his main field of activity was the application of microprocessors and digital techniques for substation and generating station control and protection systems. In 1997, he joined Schweitzer Engineering Laboratories, Inc. in the position of principal research engineer. Gabriel is an IEEE Senior Member, a registered professional engineer in the Province of Québec, and has served on the Power System Relaying Committee since May 1989. He holds over six patents and is the author or coauthor of several papers in the fields of signal processing and power networks protection and control.